

# JOURNAL OF THE AMERICAN CHEMICAL SOCIETY

© Copyright 1987 by the American Chemical Society

VOLUME 109, NUMBER 18

SEPTEMBER 2, 1987

## Furanose Ring Conformation: The Application of ab Initio Molecular Orbital Calculations to the Structure and Dynamics of Erythrofurano- and Threofuranose Rings

Anthony S. Serianni\*<sup>†</sup> and Daniel M. Chipman<sup>†</sup>

Contribution from the Department of Chemistry and the Notre Dame Radiation Laboratory, University of Notre Dame, Notre Dame, Indiana 46556. Received November 24, 1986

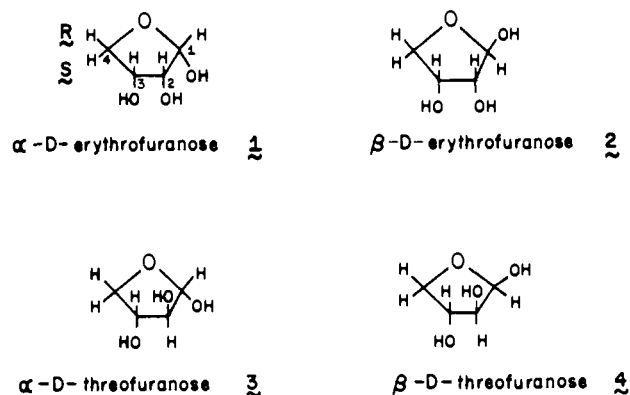
**Abstract:** Ab initio molecular orbital calculations have been conducted on four tetrahydrofuranose anomers,  $\alpha$ - and  $\beta$ -D-erythrofurano- and  $\alpha$ - and  $\beta$ -D-threofuranose, to study the effect of ring conformation on molecular parameters (bond lengths, bond angles, bond torsions) and on total energies. Geometric optimizations of envelope and planar conformers were conducted using the STO-3G basis set; single-point calculations were also performed with the 3-21G basis set. Preferred solution conformations deduced from previous NMR studies are in good agreement with those predicted by calculation, indicating that the intrinsic structures of these furanoses dictate their preferred geometries, and that solvation by water ( $^2\text{H}_2\text{O}$ ) does not appear to be a major conformational determinant. The  $\beta$ -D-erythro configuration, which is structurally related to the  $\beta$ -D-ribo configuration found in RNA, was found to have significantly different conformational behavior from the other three configurations.

Furanose rings are important components of nucleic acids and are responsible in part for the structure, conformation, and dynamics of these biopolymers. The inherent flexibility of these rings, that is, their ability to assume twist (T) and envelope (E) conformations (Figure 1) with relative ease (i.e., with relatively low activation barriers), is a well-recognized property, and interconversion between these conformers can occur via a cyclic pathway (a pseudorotational itinerary<sup>1,2a</sup>) that does not involve the planar form (Figure 2). Alternatively, interconversion between any two conformers can take place via the planar form, a process called inversion. The relative importance of these two mechanisms of conformer interconversion is still a subject of debate.<sup>2b</sup>

The conformation and dynamics of the furanose rings of ribo- (RNA) and deoxyribonucleic (DNA) acids play an important role in determining the solution behavior of these macromolecules. For example, the ability of DNA to assume different conformations (e.g., A, B, and Z forms) depends in part on the flexible furanose component. An understanding of the energetics of DNA and RNA conformational interconversion requires an assessment of furanose ring dynamics.

Despite recognition of these facts, the conformational and dynamic properties of furanose rings and how they are affected by structure and solvation are not fully understood. Conformational preferences in solution can sometimes be deduced from an analysis of vicinal  $^1\text{H}$ - $^1\text{H}$  spin couplings,<sup>3,4</sup> an approach which is improved when vicinal  $^{13}\text{C}$ - $^1\text{H}$  and  $^{13}\text{C}$ - $^{13}\text{C}$  couplings are also considered.<sup>5,6</sup> However, because of the complexity of the system, NMR provides little information on the relative energies of potential puckered forms. This information, at least for gas-phase structures (i.e., isolated unsolvated molecules), can be obtained

Scheme I



in principle from calculational methods.

We have performed ab initio molecular orbital (MO) calculations on the simplest aldofuranose rings,  $\alpha$ - and  $\beta$ -D-erythrofurano- (1, 2) and  $\alpha$ - and  $\beta$ -D-threofurano- (3, 4) (Scheme I). The conformational behavior of 1-4 and their methyl glycosides in  $^2\text{H}_2\text{O}$  has been studied previously by  $^1\text{H}$  and  $^{13}\text{C}$  NMR,<sup>5</sup> and an important aim of this study is to compare the preferred solution conformations of 1-4 deduced by NMR with conformations

(1) Kilpatrick, J. E.; Pitzer, K. S.; Spitzer, R. *J. Am. Chem. Soc.* **1947**, *69*, 2483-2488.

(2) (a) Altona, C.; Sundaralingam, M. *J. Am. Chem. Soc.* **1972**, *94*, 8205-8212. (b) Westhof, E.; Sundaralingam, M. *Ibid.* **1983**, *105*, 970-976.

(3) Stevens, J. D.; Fletcher, H. G., Jr. *J. Org. Chem.* **1968**, *33*, 1799.

(4) Angyal, S. J. *Carbohydr. Res.* **1979**, *77*, 37.

(5) Cyr, N.; Perlin, A. S. *Can. J. Chem.* **1979**, *57*, 2504.

(6) Serianni, A. S.; Barker, R. *J. Org. Chem.* **1984**, *49*, 3292.

\* Department of Chemistry.

<sup>†</sup> Notre Dame Radiation Laboratory.

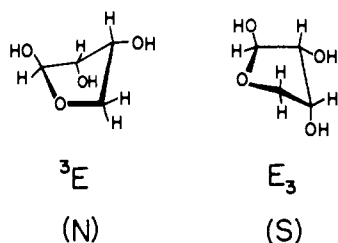


**Figure 1.** The two envelope forms of  $\beta$ -D-erythrofuranose (**2**) in which C3 is puckered out of the plane defined by C4, O4, C1, and C2. The  $^3E$  conformer is defined as having C3 "above" the ring plane, and  $E_3$  has C3 "below" the plane. The extent of puckering (puckering amplitude) can vary depending on the nature of the ring substituents. The  $^3E$  and  $E_3$  conformers are "north" (N) and "south" (S) forms, respectively, according to nomenclature used in nucleotide conformational analysis (see Figure 2).

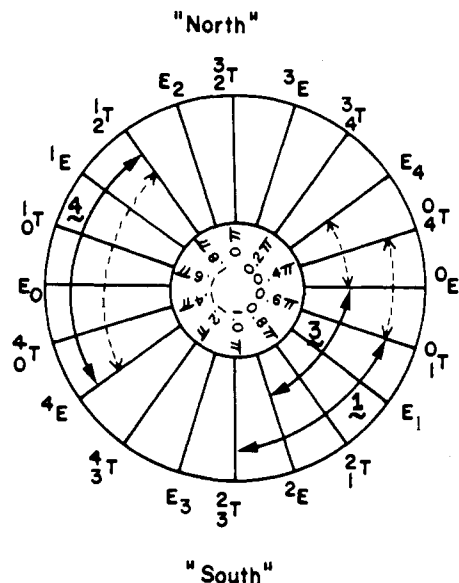


**Figure 2.** The pseudorotational itinerary<sup>1,2</sup> for furanoses, showing the pathway for the continuous interconversion of twist (T) and envelope (E) conformers. Envelope symbolisms are described in Figure 1. A  $^3T$  conformer is defined as having C4, O4, and C1 coplanar, and C2 and C3 displaced equally "below" and "above" this plane; unequal displacement of C2 and C3 is denoted by  $^3T_2$  symbolism. "North" and "south" hemispheres are identified, and the relationship between phase angle of pseudorotation and ring conformation (e.g.,  $^3T$  corresponds to a phase angle of  $0\pi$ ) is given. The preferred regions of the itinerary for **1**, **3**, and **4** in  $^2H_2O$ , as determined from NMR studies,<sup>6</sup> are indicated by solid arrows; preferred regions determined from MO calculations are indicated by dashed arrows.

predicted for "gas-phase" molecules by ab initio calculations. The results of this investigation have implications for nucleic acid structure, as compounds **1** and **2** can be considered "parent" furanoses which upon  $CH_2OH$  substitution at C4 generate furanoses having the biologically important D-ribo configuration.

Calculations have been performed on conformers (10 envelope, 1 planar) of each tetrahydrofuranose ring. In contrast to previous studies, we have not constrained these calculations with fixed bond lengths or by making assumptions about the magnitudes of the various structural forces that affect furanose conformation.<sup>7,8a</sup> Geometric optimization was complete except for a single endocyclic torsion angle (two angles in the case of planar forms), which was set at  $0^\circ$  to limit the calculation to a particular envelope conformer (Figure 1). As a consequence, we have been able to assess the relationships between ring configuration, ring conformation, and conformational energies, and evaluate the effect of conformation on structural parameters (i.e., bond lengths, angles, and torsions).

(7) Levitt, M.; Warshel, A. *J. Am. Chem. Soc.* **1978**, *100*, 2607.

(8) (a) Olson, W. K. *J. Am. Chem. Soc.* **1982**, *104*, 278. (b) Westhof, E.; Sundaralingam, M. *Ibid.* **1980**, *102*, 1493-1500.

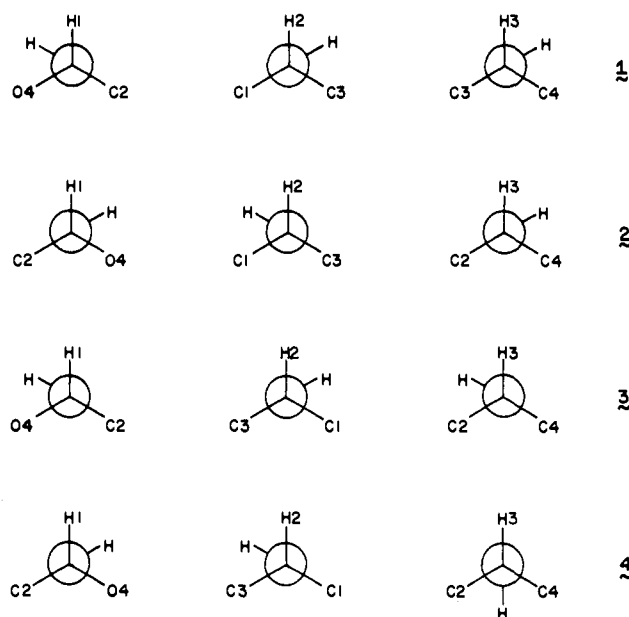


**Figure 3.** The initial exocyclic C-O rotamers used for conformational energy calculations on **1-4**. The C1-O1 rotamers were chosen to optimize the "exoanomeric effect".<sup>16</sup>

We have found that many furanose ring structural parameters are affected by conformation, that the response of these parameters to conformation reveals the presence of important structural forces, and, perhaps most important, that similar preferred geometries are suggested by NMR and ab initio methods.

#### Experimental Section

The Gaussian 80 program,<sup>9</sup> as implemented on an IBM 370/3033 mainframe computer at the Notre Dame Computing Center, was used for all calculations. Most of the calculations were performed with the minimal STO-3G basis set;<sup>10</sup> several were conducted with the split-valence 3-21G basis set.<sup>11</sup> Computations were performed on five envelope (E) forms, each with one endocyclic bond torsion fixed at  $0^\circ$ , while the remaining molecular parameters were optimized by analytic gradient methods; for planar forms, two endocyclic torsions were fixed at  $0^\circ$ . Initial estimates of structural parameters (bond lengths, angles, and torsions) were made by inspection of crystallographic data.<sup>12</sup> Geometry optimizations with the STO-3G basis set required about 6 cpu hours per structure.

A potential problem with theoretical calculations on sugars is the choice of C-O bond rotamers for hydroxyl groups in the molecule.<sup>13</sup> It was impractical to investigate every potential local minimum geometry, as this would require 27 optimizations for each conformer of **1-4**. Consequently, we chose initial C-O rotamers by model inspection with the aim of minimizing intramolecular hydrogen bonding and optimizing stereoelectronic effects at C1. These geometries are shown in Figure 3. The implications of this approach, as well as some limited exploration of other rotamers, are discussed in some detail in the Results section.

The relationship between furanose ring conformation and the phase angle of pseudorotation ( $P$ )<sup>2</sup> is illustrated in Figure 2, where, for example, the  $^3E$  conformation (Figure 1) corresponds to  $P = 0.1\pi$ . To simplify the presentation of data, conformers are identified by  $P/\pi$ , the  $^3E$  conformer corresponding to a value of  $P/\pi = 0.1$ ,  $E_4$  to a value of 0.3, and so forth.

(9) Binkley, J. S.; Whiteside, R. A.; Krishnan, A.; Seeger, R.; DeFrees, D. J.; Schlegel, H. B.; Topiol, S.; Khan, L. R.; Pople, J. A. *QCPE* **1981**, *13*, 406.

(10) (a) Hehre, W. J.; Stewart, R. F.; Pople, J. A. *J. Chem. Phys.* **1969**, *51*, 2657. (b) Newton, M. D.; Latham, W. A.; Hehre, W. J.; Pople, J. A. *Ibid.* **1970**, *52*, 4064.

(11) Binkley, J. S.; Pople, J. A.; Hehre, W. J. *J. Am. Chem. Soc.* **1980**, *102*, 939.

(12) (a) Barragán, I.; López-Castro, A.; Márquez, R. *Acta Crystallogr., Sect. B* **1977**, *33*, 2244-2248. (b) Barragán, I.; López-Castro, A.; Márquez, R. *Ibid.* **1978**, *34*, 295-298.

(13) (a) For a discussion of this problem, see: Burkert, U.; Allinger, N. L. *Molecular Mechanics*, ACS Monograph No. 177; American Chemical Society: Washington, D.C., 1982; pp 257-265. (b) Lesyng, B.; Saenger, W. *Carbohydr. Res.* **1984**, *133*, 187-197.

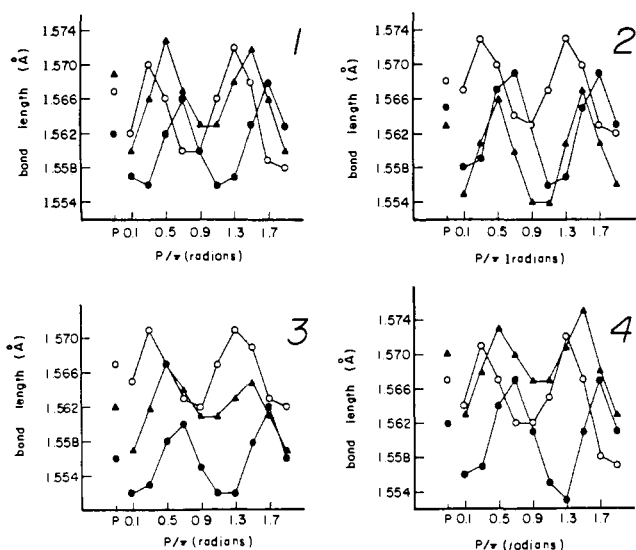


Figure 4. The effect of ring conformation of 1-4 on furanose ring endocyclic C-C bond lengths: C1-C2 (O), C2-C3 (▲), C3-C4 (●). Data were obtained using the STO-3G basis set.

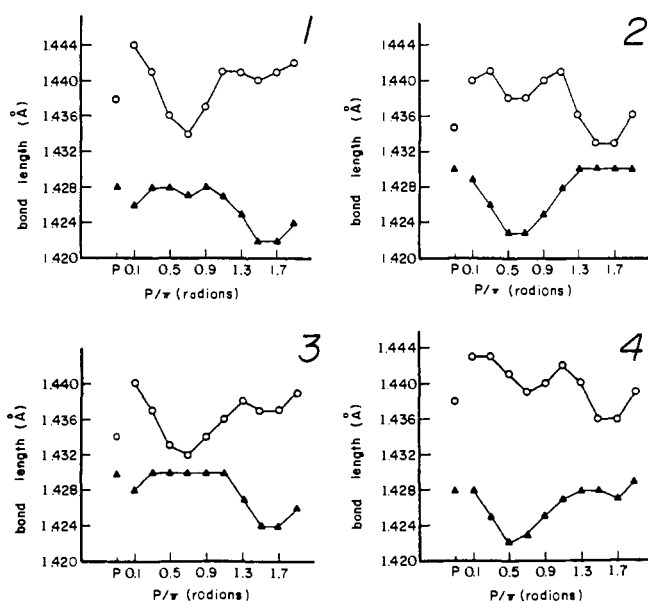


Figure 5. The effect of ring conformation of 1-4 on furanose ring C-O bond lengths: endocyclic O4-C1 (O), exocyclic C1-O1 (▲). Data were obtained using the STO-3G basis set.

## Results

**A. Bond Lengths.** Several bond lengths appear to be sensitive to furanose conformation, as shown in Figures 4-6. While it is probable that an STO-3G treatment will not give quantitatively reliable geometries, the calculated *changes* are likely to be semi-quantitatively correct. The calculated response of these bond lengths to ring conformation is found to be consistent and independent of ring configuration, lending credibility to the observed patterns.

The three endocyclic C-C bonds of 1-4 experience similar cyclical changes in length (Figure 4) by about 0.01 to 0.02 Å. For example, the C1-C2 bond (see atom numberings in Scheme I) of 3 is longest at 0.3 and 1.3  $P/\pi$ , and shortest at 0.9 and 1.9  $P/\pi$ . The C2-C3 and C3-C4 bonds show similar behavior, but with maxima and minima shifted, respectively, by 0.2  $P/\pi$ . Similar trends are observed for 1, 2, and 4 (Figure 4).

The endocyclic C1-O4 bond changes in length by about 0.01 Å with ring conformation (Figure 5). In contrast to endocyclic C-C bonds, the response of the endocyclic C1-O4 bond to ring conformation (Figure 5) also depends on anomeric configuration. For  $\alpha$  anomers (1, 3), the C1-O4 bond is shortest at 0.7  $P/\pi$ , with

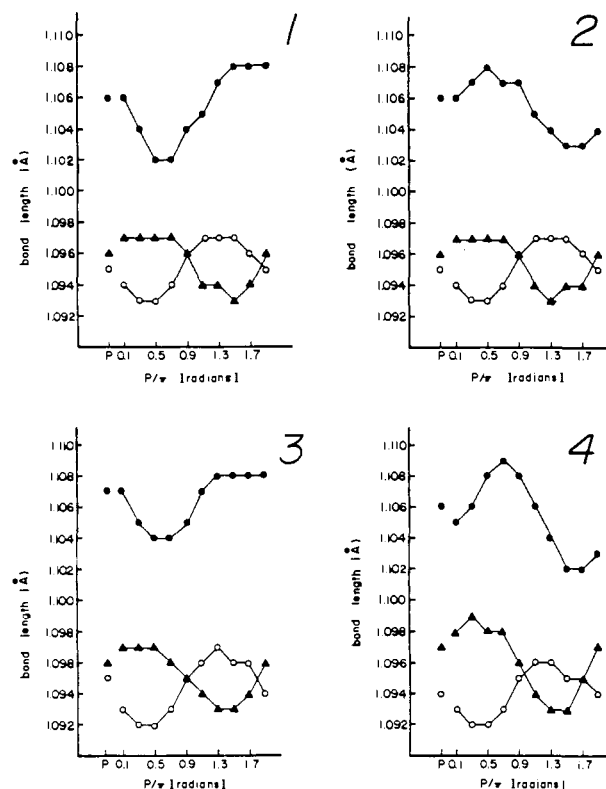


Figure 6. The effect of ring conformation of 1-4 on furanose ring C-H bond lengths: C1-H1 (●), C4-H4R (O), C4-H4S (▲). Data were obtained using the STO-3G basis set.

a second less defined local minimum found at 1.5-1.7  $P/\pi$ . The same overall pattern is found for  $\beta$  anomers (2, 4), but minima are reversed; that is, the C1-O4 bond is shortest at 1.5  $P/\pi$  and the local minimum occurs at 0.7  $P/\pi$ . In general, the response of the C4-O4 bond length to conformation is similar in 1-4 (data not shown), with minima at 0.3-0.5  $P/\pi$  and 1.3-1.5  $P/\pi$ .

The exocyclic C1-O1 bond length also is sensitive to conformation (Figure 5), changing by about 0.01 Å. In  $\alpha$  anomers, the C1-O1 bond is shortest at 1.5-1.7  $P/\pi$ , and longest over a broad range of conformers extending from 0.3 to 1.1  $P/\pi$ . The C2-O2 and C3-O3 bond lengths are not significantly affected by ring conformation.

The lengths of C-H bonds in the vicinity of the ring oxygen vary with ring conformation (Figure 6) by nearly 0.01 Å. The C1-H1 bond in  $\alpha$  anomers is shortest at 0.5-0.7  $P/\pi$  and longest at 1.3-1.9  $P/\pi$ . The opposite is found for  $\beta$  anomers, in which C1-H1 is shortest at 1.5-1.7  $P/\pi$  and longest at 0.5-0.7  $P/\pi$ . The methylene C4-H4R and C4-H4S bonds are also notably affected by conformation in a uniform manner in all four structures. C4-H4R bonds (see Scheme I for R and S assignments) are shortest at 0.3-0.5  $P/\pi$  and longest at 1.1-1.5  $P/\pi$ ; opposite and complementary curves are found for C4-H4S (Figure 6). In general, C2-H2 and C3-H3 bonds are not significantly affected by conformation, with the possible exception of C2-H2 of 4 (data not shown).

**B. Bond Angles.** The endocyclic bond angles of  $\beta$ -D-ribofuranose have been shown by De Leeuw et al.<sup>14</sup> using FF-2 force field methods to depend on the phase angle of pseudorotation. Ab initio (STO-3G) calculations on the tetrafurans 1-4 reveal the same general trends (Figure 7). The calculated CCC bond angles ( $101-104^\circ$ ) are smaller than the CCO and COC bond angles ( $105-110^\circ$ ), which is consistent with angle bending forces.<sup>15</sup> Furthermore, the cyclical pattern of angle changes is independent of ring configuration; that is, erythro 1, 2 and threo 3, 4 structures

(14) DeLeeuw, H. P. M.; Haasnoot, C. A. G.; Altona, C. *Isr. J. Chem.* **1980**, *20*, 108-126.

(15) Westheimer, F. *Steric Effects in Organic Chemistry*; Newman, M. S., Ed.; Wiley: New York, 1956; Chapter 12, pp 523-555.

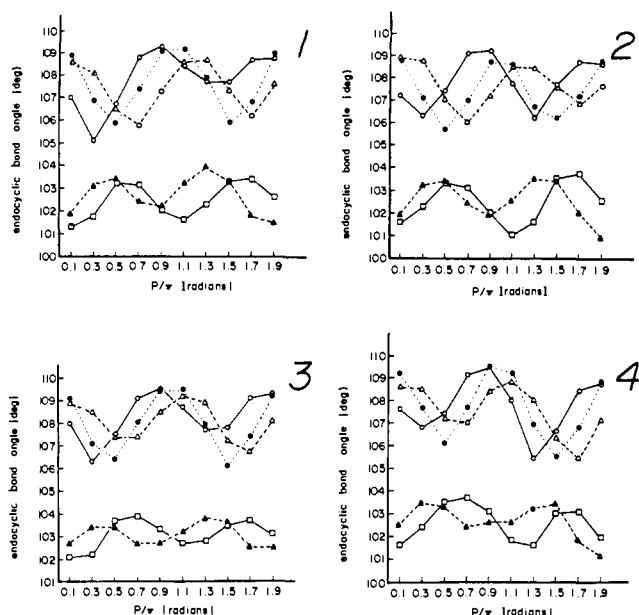


**Figure 7.** The effect of ring conformation of 1-4 on furanose ring endocyclic bond angles: C1-C2-C3 (▲), C2-C3-C4 (□), C3-C4-O4 (○), C4-O4-C1 (●), O4-C1-C2 (Δ). Data were obtained using the STO-3G basis set.

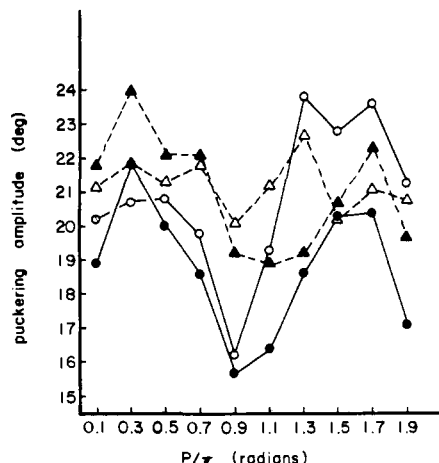


**Figure 8.** The effect of ring conformation of 1-4 on furanose ring pucker amplitude: 1 (▲), 2 (Δ), 3 (●), 4 (○). Data were obtained using the STO-3G basis set.

show similar behavior. One exception may be the C3-C4-O4 bond angle; a well-defined minimum occurs at 1.3  $P/\pi$  in  $\alpha$  anomers but not in  $\beta$  anomers. The observed dependence of endocyclic bond angle on ring conformation shown in Figure 7 agrees qualitatively with that reported by Olson<sup>8a</sup> and Westhof and Sundaralingam.<sup>8b</sup> However, the amplitudes of the curves derived by Westhof and Sundaralingam<sup>8b</sup> for furanose rings with  $\tau_m = 20^\circ$  (like 1-4) are considerably smaller than those found in this study.

**C. Bond Torsions.** The puckering amplitude of tetrahydrofuranose rings varies with conformation (Figure 8), most notably for 1, 3, and 4. Calculated puckerings of 16 to 24° were obtained depending on ring configuration and conformation. For 1, 3, and 4, the overall shape of the pucker amplitude-conformation curve is conserved, with minimal puckering occurring at  $\sim 1.0 P/\pi$ .  $\beta$ -D-Erythrofurano-2 behaves differently, however, having a somewhat flatter response of puckering to conformation. These data, at least for 1, 3, and 4, are inconsistent with a "circular" pseudorotational pathway in which the puckering amplitude remains constant for all envelope conformers.

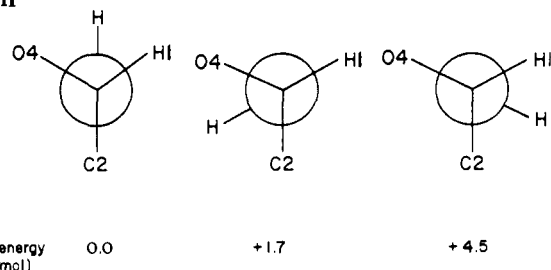
As mentioned in the Experimental Section, the choice of C-O rotamers for the hydroxyl groups in 1-4 can affect the results of theoretical calculations of preferred geometries of sugars.<sup>13</sup> It

**Table I.** Effect of OH Orientation on the Relative Energy<sup>a</sup> of  $\alpha$ -D-Threofuranose 3 in the  $E_4$  Conformation

hydroxyl conformation O1, O2, O3	energy difference (kcal/mol)
-60, 60, -60	0.0 <sup>b</sup>
60, 60, -60	4.5
180, 60, -60	1.7
-60, -60, -60	1.5
-60, 180, -60	0.9
-60, 60, 60	0.9
-60, 60, 180	0.9
-60, -60, 180	0.4
-60, -60, 60	0.5
-60, 180, 60	1.9
-60, 180, 180	1.4

<sup>a</sup> From STO-3G optimization. <sup>b</sup> The calculated total energy of this conformer was -282 166.7 kcal/mol.

**Scheme II**



is important to note that the C1-O1 torsion in 1-4 is not structurally equivalent to the C2-O2 and C3-O3 torsions, the former being subject to the "exoanomeric effect"<sup>16</sup> whereby the lone-pair electrons on O1 and the ring oxygen control stereoelectronically the C1-O1 torsion. Ab initio calculations on smaller molecules<sup>17</sup> and NMR studies of monosaccharides<sup>18</sup> have shown that, in general, the hydrogen attached to O1 prefers to orient antiperiplanar to C2 (i.e., gauche to H1 and the ring oxygen).

To explore the effect of C-O rotamers on total energies,  $\alpha$ -D-threofuranose 3 was optimized in all 10 envelope conformations using each of the three initial C-O rotamers shown in Figure 3. Compound 3 was chosen because the three hydroxyl groups are oriented trans in this molecule, and hydrogen bonding between them for any combination of ring and C-O conformations is structurally forbidden. Under these conditions,  $E_4$  was found to be the most stable envelope conformer. To evaluate the effect of C1-O1 torsion angle on total energy, three geometric optimizations of 3 in the  $E_4$  conformation were conducted with the same initial structural parameters except for the C1-O1 torsion, which was chosen to inspect the three potential staggered conformations. The relative energies of the resulting three optimized structures are given in Table I. The results show that the most preferred C1-O1 rotamer is that having the hydroxyl hydrogen anti to C2 (Scheme II); the least preferred (4.5 kcal/mol higher in energy) places the hydrogen on O1 anti to the ring oxygen. These results are consistent with previous theoretical studies on smaller structures,<sup>17</sup> and provide support for the "exoanomeric effect"<sup>16</sup> in furanoses.

Assuming that the preferred C1-O1 rotamer in the  $E_4$  conformer of 3 is independent of C2-O2 and C3-O3 rotamers, calculations were performed on 3 in the  $E_4$  conformation in which the initial C1-O1 rotamer was held constant at the most stable "exoanomeric" conformation, and the structure was reoptimized using all possible combinations of C-O rotamers at C2 and C3. The energies of these structures (Table I) are notably affected by C2 and C3 hydroxyl torsions. It is important to note that the initial C-O rotamers shown in Figure 3 for 3 produce the most

(16) Lemieux, R. U. *Pure Appl. Chem.* 1971, 25, 527.

(17) Jeffrey, G. A.; Pople, J. A.; Binkley, J. S.; Vishveshwara, S. *J. Am. Chem. Soc.* 1978, 100, 373-379.

(18) Dais, P.; Perlin, A. S. *Can. J. Chem.* 1982, 60, 1648-1656.

Table II. Comparison of Molecular Parameters for the E<sub>4</sub> Conformer of  $\alpha$ -D-Threofuranose **3** and Methyl  $\alpha$ -D-Threofuranoside

	bond lengths					bond angles					bond torsions			
	STO-3G	3-21G	STO-3G	STO-3G		STO-3G	3-21G	STO-3G	STO-3G		STO-3G	3-21G	STO-3G	STO-3G
R12	1.562 <sup>a</sup>	1.533 <sup>b</sup>	1.561 <sup>c</sup>	1.564 <sup>d</sup>	A123	102.2 <sup>a</sup>				T3451	21.8 <sup>a</sup>	25.4 <sup>b</sup>	22.1 <sup>c</sup>	27.0 <sup>d</sup>
R23	1.553				A234	106.3				T4512	0.0	0.0	0.0	6.4
R34	1.438	1.453	1.438	1.438	A345	107.1	107.7 <sup>b</sup>	107.2 <sup>c</sup>	106.6 <sup>d</sup>	T3456	142.0	145.9	142.5	147.2
R45	1.437	1.428	1.437	1.436	A451	108.5	106.5	108.4	108.2	T3457	96.7	90.5	96.0	91.4
R51	1.571	1.540	1.572	1.571	A512	103.4	103.9	103.4	103.5	T6578	67.4	70.5	56.1	66.3
R56	1.105	1.077	1.104	1.104	A456	107.2	107.6	107.2	107.1	T4519	115.9	115.9	115.9	122.4
R57	1.430	1.418	1.432	1.430	A457	111.0	110.7	111.8	111.2	T45110	119.0	117.7	119.1	112.5
R78	0.990	0.967	1.438	0.990	A578	104.0	110.3	110.2	104.0	T911011	53.2	47.9	53.6	54.0
R19	1.097	1.080	1.097	1.097	A519	107.9	108.1	107.9	108.0	T51212	96.3	92.7	96.0	101.6
R110	1.430	1.435	1.430	1.430	A5110	114.4	114.1	114.4	114.3	T51213	138.5	141.6	138.8	133.4
R1011	0.990	0.966	0.990	0.990	A11011	104.4	111.1	104.4	104.4	T1221314	54.1	51.2	54.7	53.8
R212	1.097	1.082	1.097	1.097	A1212	108.0	107.1	108.1	108.0	T54315	156.7	161.2	157.0	158.4
R213	1.430	1.429	1.429	1.430	A1213	114.6	114.5	114.6	114.5	T54316	83.7	76.4	83.4	81.9
R1314	0.991	0.966	0.991	0.990	A21314	104.4	110.6	104.0	104.1	T717818			120.0	
R315	1.092	1.076	1.092	1.092	A4315	108.5	108.5	108.4	108.5	T717819			120.0	
R316	1.097	1.080	1.097	1.097	A4316	111.7	111.3	111.7	111.7					
R817			1.095		A7817									
R818			1.094		A17818									
R819			1.090		A17819									

<sup>a</sup> Parameters for **3** obtained from STO-3G optimization. The symbols "R", "A", and "T" denote bond lengths, bond angles, and bond torsions between the indicated atoms according to the numbering system shown in Scheme III. <sup>b</sup> Parameters for **3** obtained from 3-21G optimization. <sup>c</sup> Parameters for methyl  $\alpha$ -D-threofuranoside obtained from STO-3G optimization; atom numberings as shown in Scheme III. For the glycoside, the methyl carbon is atom 8, and the methyl hydrogens are atoms 17-19. <sup>d</sup> Parameters obtained after release of the T4512 constraint and STO-3G reoptimization using the initial parameters in (a); these parameters correspond to a twist (<sup>0</sup>T<sub>2</sub>) form (see text).

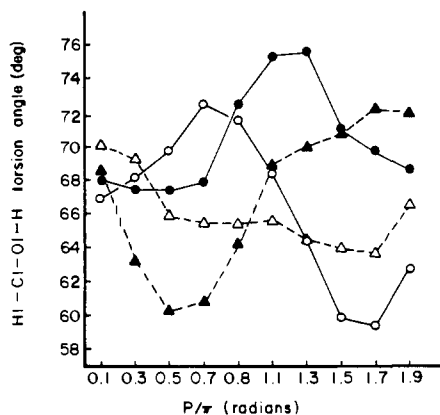


Figure 9. The effect of ring conformation of **1-4** on the H1-C1-O1-H torsion angle: **1** ( $\blacktriangle$ ), **2** ( $\triangle$ ), **3** ( $\bullet$ ), **4** ( $\circ$ ).

stable E<sub>4</sub> conformer of **3**. We have not determined whether the initial C2-O2 and C3-O3 rotamers used for energy calculations on **1**, **2**, and **4** (Figure 3) represent optimal energy conformations, but the "exoanomeric effect"<sup>16</sup> was optimized for C1-O1 torsions in these molecules (Figure 3). In any case, it is reasonable to propose that overall trends will be conserved regardless of whether lowest energy structures (in terms of hydroxyl group conformations at C2 and C3) were chosen to conduct the computations.

The torsion angle defined by H1-C1-O1-H in the optimal "exoanomeric" conformation is sensitive to ring conformation and anomeric configuration (Figure 9), varying over a range of 14°. Curves for **1**, **3**, and **4** show defined minimal and maximal angles, while that for **2** appears flatter and less responsive to ring conformation.

**D. Conformational Energy Calculations.** The 10 envelope forms and the planar form of **1-4** having initial exocyclic C-O rotamers shown in Figure 3 were optimized using Gaussian 80<sup>9</sup> and the STO-3G basis set,<sup>10</sup> and total energies were obtained (Figure 10). Single-point calculations with the more flexible 3-21G basis set<sup>11</sup> were also performed for each conformer using the optimized structural parameters obtained from the STO-3G calculations, and curves generated from these data are also given in Figure 10. In one case (**3**), the geometries of the lowest and highest energy conformers were reoptimized with the 3-21G basis set to compare the energy difference with that obtained with the STO-3G basis set, and to evaluate the effect of this split-valence basis set on optimized molecular parameters (Table II).

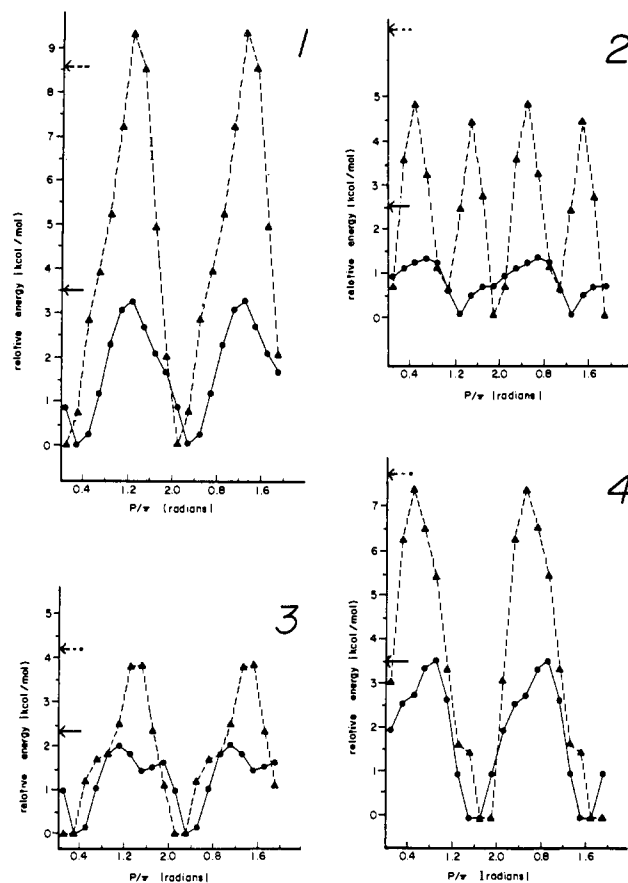
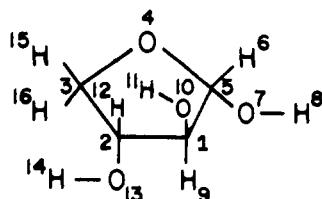


Figure 10. The effect of ring conformation of **1-4** on relative energy, determined by optimization with the STO-3G basis set ( $\bullet$ ) and by single-point calculations with the 3-21G basis set ( $\blacktriangle$ ) using STO-3G optimized parameters. The arrows indicate STO-3G ( $\leftarrow$ ) and 3-21G ( $\leftarrow$ ) energies of planar forms. Two complete cycles of the pseudorotational itinerary are shown.

For **1**, **3**, and **4**, the overall shapes of the energy profiles (Figure 10) obtained by STO-3G optimization are generally similar to those obtained from the single-point 3-21G calculations performed with STO-3G optimized parameters, although the 3-21G energy differences are consistently somewhat larger than those determined by STO-3G calculations. These profiles are characterized by the

Scheme III



presence of a global minimum; that is, they indicate the existence of a single lowest energy conformer. However, the STO-3G and 3-21G curves for  $\beta$ -D-erythrofurano-2 differ considerably. In this case, the STO-3G data do not support a definite minimum energy conformer, whereas the 3-21G data indicate two well-defined conformational minima at 0 and 1  $P/\pi$ .

**E. Effect of Glycosidation on Furanose Structural Parameters.** STO-3G optimization was conducted on the glycoside, methyl  $\alpha$ -D-threofuranoside, in the  $E_4$  conformation (chosen because  $E_4$  is the lowest energy conformer of the corresponding reducing sugar,  $\alpha$ -D-threofuranose **3**) to evaluate the effect of the methyl glycosidation on structural parameters. A comparison of results is found in Table II. No significant changes in bond lengths and angles are observed upon glycosidation, including those involving the anomeric carbon, and the puckering amplitude is essentially unaltered in both structures (Table II). The C1–O1 torsion angle (the “exoanomeric” torsion<sup>16</sup>) is smaller in the glycoside ( $56^\circ$  in the glycoside,  $67^\circ$  in the reducing sugar), which positions the methyl aglycone further away from the ring atoms, apparently to reduce steric interactions.

**F. Effect of Basis Set on Optimized Structural Parameters.** The  $E_4$  conformer of **3** was optimized with the STO-3G and 3-21G basis sets to evaluate the effect on calculated structural parameters (Table II). C–C bond lengths are shorter by  $\sim 0.03$  Å with the 3-21G basis set. C–O bond lengths involving the ring and anomeric oxygens also appear to be affected by basis set; in the STO-3G calculations, C1–O4  $\approx$  C4–O4  $>$  C1–O1, whereas in 3-21G, C4–O4  $>$  C1–O4  $>$  C1–O1. In general, C–H bonds are shorter by  $\sim 0.02$  Å in 3-21G calculations.

The most significant difference in bond angles occurs for C–O–H angles, which are  $\sim 104$  and  $\sim 110^\circ$  for STO-3G and 3-21G calculations, respectively. A related observation has been made for the H–O–H angle of water, which is calculated to be  $100.0^\circ$  (STO-3G)<sup>10b</sup> and  $107.6^\circ$  (3-21G),<sup>11</sup> bracketing experiment ( $104.5^\circ$ ). Also noteworthy is the difference in the relative magnitudes of the endocyclic COC, CCO, and CCC bond angles calculated from the STO-3G and 3-21G basis sets. In the STO-3G treatment, CCO  $>$  COC  $>$  CCC, whereas in the 3-21G treatment, COC  $>$  CCO  $>$  CCC. The latter relationship is more consistent with experimental data.<sup>15</sup> Because of the error in the oxygen valence angles, there will be inherent uncertainties in the study of furanose ring structure using the STO-3G basis set.

Calculated bond torsions also depend on the basis set used. For example, puckering amplitudes (Table II, T3451) are somewhat larger for 3-21G optimized rings; most of the other observed differences in torsion angles result from this altered puckering amplitude.

## Discussion

The ab initio MO calculations performed in this study demonstrate that the fundamental structural properties of the furanose ring (bond lengths, angles, torsions) depend on ring conformation. Whereas previous theoretical studies have concentrated on the  $\beta$ -ribo configuration for obvious biological reasons, we have studied four configurations, **1–4**, with the belief that a comparison of these configurations might reveal important information about furanose structure and dynamics in general. In the four compounds studied, furanose structural properties were found to respond systematically to molecular shape. It should be emphasized that the *absolute* values or changes predicted from STO-3G calculations are not to be considered quantitatively reliable. However, the *general trends* revealed by these calculations are internally consistent in the four furanose configurations, and are expected to correctly reflect the behavior of these molecules in the gas phase. We

discuss the implications of these calculations for solvated molecules later.

It is particularly interesting to evaluate how structure at the anomeric center of furanoses is affected by ring conformation, especially since the “anomeric effect”<sup>19</sup> is considered to be an important determinant of furanose ring conformation.<sup>4–6</sup> From a comparison of Figures 5, 6, and 10, the C1–H1 and O4–C1 bonds are shortest and the C1–O1 bond longest in the most stable ring conformers of **1**, **3**, and **4**. The apparent exception is **2**, although a similar result might be obtained if optimizations of envelope conformers were conducted with the 3-21G basis set in this case.

The behavior of the methylene C–H bond lengths (C4–H4R, C4–H4S) (Figure 6) can be rationalized by noting their relative orientation with respect to the lone-pair orbitals of the ring oxygen as a function of ring conformation. The response of these bonds to conformation is identical in **1–4**, indicating that ring configuration does not play an important role in the observed dependence. It appears that these C–H bonds increase in length as they become more antiperiplanar to a lone-pair orbital on the ring oxygen. In light of this apparent effect, it is noteworthy that the C4–H4R and C4–H4S bonds of **1–4** show different one-bond <sup>13</sup>C–<sup>1</sup>H couplings<sup>6</sup> and different chemical reactivities,<sup>20</sup> behavior that may be attributed to small but important bond-length differences. A similar effect of ring conformation on C1–H1 bond length (Figure 6) was noted above, and may also be attributed to the same lone-pair orbital effect by the ring oxygen.

With respect to relative length, the C1–H1 bond in **1–4** is the longest C–H bond in these molecules (Figure 6). The <sup>1</sup>H NMR signals of the anomeric protons of **1–4** (and of anomeric protons in general) are found well downfield of those of the remaining protons in these structures,<sup>6</sup> suggesting that bond length, in addition to electronegativity effects, may be a determinant of <sup>1</sup>H chemical shieldings; that is, as C–H bonds increase in length, <sup>1</sup>H signals shift further downfield. A similar observation was made recently from ab initio calculations on aldo-1,4-lactones.<sup>21</sup>

Further support of an “exoanomeric effect”<sup>16</sup> in furanoses has been provided by these calculations. The preferred orientation of the hydrogen on O1 of **3** is consistent with that found in simpler molecular fragments by experiment and computation.<sup>17,18</sup>

The calculated puckering amplitudes of **1–4** ( $\sim 20^\circ$ ) are smaller than those found by X-ray crystallography for the  $\beta$ -D-ribofuranose constituent of ribonucleosides ( $\sim 40^\circ$ ).<sup>14</sup> This difference may be attributed to the presence of a bulkier hydroxymethyl substituent at C4 of  $\beta$ -D-ribofuranose which is better accommodated in a more puckered ring. The smaller puckering angles in **1–4**, however, may be an artifact of the calculational method, as STO-3G calculations are known to give smaller furanose ring puckerings than are found experimentally.<sup>22,23</sup> Glycosidation does not appear to alter the puckering amplitudes of furanoses.

A major objective of this study was to compare preferred “gas-phase” geometries predicted by ab initio calculations with those determined in solution (<sup>2</sup>H<sub>2</sub>O) by NMR methods. The calculated lowest energy conformations of **1**, **3**, and **4** (Figure 10) are similar to (but not identical with) the preferred solution (<sup>2</sup>H<sub>2</sub>O) conformations of these molecules (Figure 2). In both the gas and solution phases, the “anomeric effect”<sup>19</sup> is an important determinant of furanose ring conformation. NMR spin couplings in **1**, **3**, and **4**<sup>6</sup> provide evidence that these molecules prefer conformations in solution in which the C1–O1 bond is quasi-axial (or near quasi-axial), as predicted from this effect. The MO calculations indicate similar conformations (Figure 2), suggesting that solvation by water does not appreciably alter preferred conformation. In other words, the intrinsic structures of **1**, **3**, and **4** dictate in large part their preferred geometries, and solvation

(19) Lemieux, R. U. *Molecular Rearrangements*; de Mayo, P., Ed.; Wiley-Interscience: New York, 1963; p 713.

(20) Wu, G. D.; Serianni, A. S.; Barker, R. *J. Org. Chem.* **1983**, *48*, 1750–1757.

(21) Angelotti, T.; Krisko, M.; O'Connor, T.; Serianni, A. S. *J. Am. Chem. Soc.*, in press.

(22) Cremer, D.; Pople, J. A. *J. Am. Chem. Soc.* **1975**, *97*, 1358–1367.

(23) Harvey, S. C.; Prabhakaran, M. *J. Am. Chem. Soc.* **1986**, *108*, 6128–6136.

by water ( $^2\text{H}_2\text{O}$ ) does not appear to be a major conformational determinant. It should be noted, however, that the agreement between NMR and MO data is not perfect, and that some contribution to preferred furanose geometry made by solvation is possible, especially for the  $\alpha$  anomers **1** and **3**. As pointed out by a reviewer, the effect of water on preferred conformation cannot be convincingly settled without explicit consideration of water in either a quantum or statistical mechanics treatment.

Most interestingly, the  $^1\text{H}$ - $^1\text{H}$  and  $^{13}\text{C}$ - $^1\text{H}$  coupling data<sup>6</sup> obtained for  $\beta$ -D-erythrofurano-**2** was found to be insufficient to assign a preferred conformation in  $^2\text{H}_2\text{O}$ . Indeed, as stated earlier,<sup>6</sup> **2** appears to assume more than one "stable" conformation in aqueous solution. The MO calculations, at least with the 3-21G basis set, support this conclusion. Angyal<sup>24</sup> has suggested, based on  $^1\text{H}$ - $^1\text{H}$  spin couplings, empirical observations and model inspection, that **2** interconverts between two conformers, namely,  $^2\text{T}_3$  and  $^3\text{T}_2$ . These are the same conformers found to be most stable by MO calculations (Figure 10). Of the four ring configurations studied,  $\beta$ -D-erythrofurano-**2**, which is structurally related to the  $\beta$ -D-ribofurano- constituent of RNA, appears unique in several respects (see Figures 8, 9, and 10). Most notably, this structure can assume two relatively stable conformers, apparently similar to  $\beta$ -D-ribofurano-<sup>8a,23</sup> It is not inconceivable that this configuration is the most energetically suitable for these biopolymers, being more able to assume significantly different "north" and "south" conformers (Figure 2) in order to accommodate a different polymer conformation required for a given biological process (i.e., RNA-protein binding).

Because of the uncertainties inherent in ab initio STO-3G MO calculations on "complex" molecules like **1-4**, the energy differences between conformers (Figure 10) cannot be considered quantitatively accurate. For example, STO-3G optimizations of **3** predict  $E_4$  and  $E_3$  to be the most and least stable *envelope* conformers, respectively, with an energy difference in 2.1 kcal/mol. Single-point calculations with the 3-21G basis set using STO-3G optimized molecular parameters indicate  $E_4$  and  $E_0$  to be most and least stable, respectively, with an energy difference of 3.9 kcal/mol; 3-21G geometry optimization increases this difference to 4.3 kcal/mol. The planar form of **3** is less stable than the envelope conformers, but the energy difference between it and the least stable envelope form is small ( $\sim 0.3$  kcal/mol). Thus, inversion cannot be excluded as a mechanism of conformer interconversion at room temperature. STO-3G optimizations and 3-21G single-point calculations do suggest that **2** and **3** interconvert between envelope conformers via pseudorotation more easily than

**1** and **4**, but this conclusion requires validation from more sophisticated calculations.

The pseudorotational pathway<sup>1,2</sup> of interconversion of furanose conformers (Figure 2) assumes that adjacent envelope forms (e.g.,  $E_2$  and  $^3E$ ) interconvert via a twist form (i.e.,  $^3T$ ). Implicit in the energy plots shown in Figure 10 is the assumption that a twist form will have an energy close to that of adjacent envelope forms; that is, these curves are smooth and continuous. We have not conducted optimizations on twist forms to verify this assumption in all cases. We have, however, conducted a calculation that supports this assumption. As shown in Table I and Figure 10, STO-3G calculations indicate that  $E_4$  is the most stable envelope form of **3**. When the endocyclic torsion angle is allowed to relax from its  $E_2$ -constrained value of  $0^\circ$  and the structure is reoptimized, a new minimum energy conformer,  $^0T_4$ , is obtained with the structural parameters given in Table II. None of the bond lengths change appreciably. The largest changes are about  $6^\circ$  in several torsions, including that previously constrained to  $0^\circ$ . This "dissymmetric" twist form (see the legend for Figure 2) is only 0.1 and 0.2 kcal/mol lower in energy than  $E_4$  and  $^0E$ , respectively, as expected if pseudorotation is continuous. These results also indicate that while twist forms rather than envelope forms may be the true lowest energy conformers of **1**, **2** and **4**, very little energy is required to convert a twist form to neighboring envelope forms.

These ab initio studies have shown that furanose rings are dynamic structures not only with respect to bond torsions (i.e., pseudorotation, inversion) but also bond lengths and angles. The present study has identified general patterns that exist between furanose ring structural parameters, ring configuration, and ring conformation. The major findings are consistent with conclusions derived from NMR coupling data, indicating that calculations such as these can provide useful information on the structural and dynamic behavior of furanose systems.

**Acknowledgment.** D.M.C. acknowledges support of this work by the Office of Basic Energy Science of the U.S. Department of Energy. This is Document No. NDRL-2922 from the Notre Dame Radiation Laboratory. A.S. acknowledges the support of this work by the Research Corporation (10028) and the National Institutes of Health (GM 33791). We thank the Notre Dame Computing Center for assistance in implementing the Gaussian 80 program and for the generous use of their facility, and Rosemary Patti for typing the manuscript.

**Registry No.** **1**, 72599-80-5; **2**, 72599-81-6; **3**, 80877-72-1; **4**, 80877-73-2.

(24) Angyal, S. J. *Carbohydr. Res.* 1979, 77, 37.

## Nonclassical Distortions at Multiple Bonds

Georges Trinquier\* and Jean-Paul Malrieu

*Contribution from the Laboratoire de Physique Quantique (C.N.R.S., U.A. No. 505), Université Paul-Sabatier, 31062 Toulouse Cedex, France. Received November 26, 1986*

**Abstract:** Both experiments and ab initio calculations exhibit cases where double bonds deviate from planarity, and cumulenones or triple bonds deviate from linearity. In a simple valence bond modelling, the occurrence and extent of these distortions are related to the singlet-triplet separation ( $\Delta E_{S-T}$ ) of the interacting fragments forming the multiple bond. This explains why inclusion of electron correlation may be so crucial for a reliable description of such deformations through quantum calculations. Various distortions are explained and others suggested for a set of unsaturated systems including alkenes, olefins, ketenes, cumulenones, allenes, ylides, and diazo compounds whenever they are built from fragments with a large  $\Delta E_{S-T}$ . Possible extensions to transition metal complexes are proposed.

Trans-bent distortions of double bonds occur in two types of strain-free unsaturated systems. The first type is the pseudoolefins  $\text{H}_2\text{X}=\text{XH}_2$ , X being a heavier analogue of carbon, i.e., Si, Ge,

and Sn. According to accurate ab initio calculations, the deviation from planarity, **1**, increases from  $\theta = 0^\circ$  for carbon, to  $\theta = 40^\circ$  for germanium or tin.<sup>1,2</sup> Disilene,  $\text{H}_2\text{Si}=\text{SiH}_2$ , is on the bor-